

Thiourea-Formaldehyde Polymer a New and Effective Corrosion Inhibitor for Mild Steel in Hydrochloric Acid Solution

Priyanka Singh¹, M.A. Quraishi^{1,*}, Eno E. Ebenso²

¹Department of Chemistry, Indian Institute of Technology, Banaras Hindu University, Varanasi-221005

²Material Science Innovation & Modelling (MaSIM) Research Focus Area, Faculty of Agriculture, Science and Technology, North-West University (Mafikeng Campus), Private Bag X2046, Mmabatho 2735, South Africa

*E-mail: maquraishi@rediffmail.com; maquraishi.apc@itbhu.ac.in

Received: 15 April 2014 / Accepted: 2 June 2014 / Published: 16 June 2014

Thiourea-Formaldehyde polymer (T-F Polymer) was synthesized by microwave method and its inhibitive action on the corrosion of mild steel (MS) in 1 M HCl was investigated under different experimental conditions using weight loss, electrochemical impedance spectroscopy (EIS) and potentiodynamic polarization technique. These techniques confirmed the adsorption of polymer on mild steel surface. Results obtained showed that the polymer acts as a good corrosion inhibitor for MS in 1 M HCl. It inhibits corrosion by adsorption mechanism. Tafel polarization data revealed that the polymer acted as mixed-type inhibitor. The adsorption of the inhibitor on mild steel surface obeyed the Langmuir adsorption isotherm.

Keywords: T-F Polymer, Mild steel, Weight loss, Electrochemical measurements, Optical microscopy

1. INTRODUCTION

The use of corrosion inhibitors is an effective and economic method for controlling corrosion of metals and alloys in many industrial processes during pickling processes, industrial acid cleaning, oil and gas well acidizing [1-3]. Organic compounds containing nitrogen, sulphur, oxygen atoms and multiple bonds act as effective corrosion inhibitors and inhibit corrosion by adsorption mechanism [4-11]. As effective corrosion inhibitors, these compounds have a strong tendency to displace water molecule from the metal surface, interact with anodic or cathodic reaction sites to retard the oxidation and reduction corrosion reaction, and prevent transportation of water and corrosion active species on

the surface. The chemical structure of the molecule (mostly planner) affects the rate of adsorption and the corrosion inhibition [12-14]. Polymers have been reported as effective corrosion inhibitors because of their high molecular weight and large size they provide high corrosion inhibition [15-20]. The Polymers having large repeating units that may cover more area on the metal surface and form a metal-polymer complex which leads to high inhibition efficiency [21]

In present work we have studied the inhibitive action of T-F polymer on corrosion of mild steel in 1 M HCl using weight loss, electrochemical impedance spectroscopy (EIS) and potentiodynamic polarization techniques.

2. EXPERIMENTAL

2.1. Materials and Solutions

Weight loss and electrochemical experiments were performed on mild steel having following composition (wt. %): 0.076% C, 0.192% Mn, 0.012% P, 0.026% Si, 0.050% Cr, 0.023% Al, 0.123% Cu and remaining Fe. For weight loss study, mild steel coupons having dimensions of 2.5 cm × 2 cm × 0.025 cm were used. For electrochemical study, coupons having dimensions of 8 cm × 1 cm × 0.025 cm with an exposed area of 1 cm² and rest being covered by epoxy resin were used as working electrode. The test solution of 1 M HCl was prepared by diluting analytical grade 37% HCl with double distilled water. The stock solution of Thiourea-Formaldehyde polymer (T-F polymer) which was used as inhibitor was prepared in a water-ethanol mixture having a ratio of 10:1.

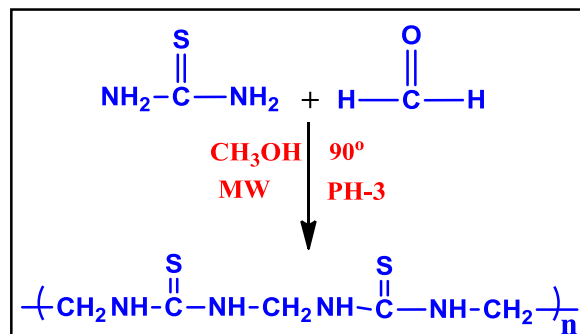
2.2. Synthesis of Thiourea-Formaldehyde polymer

Thiourea-Formaldehyde polymer (T-F polymer) was synthesized by polycondensation of thiourea and formaldehyde in acidic medium (Scheme 1). In a 100 ml three-necked round-bottomed flask, 1.52 g of Thiourea and 10 ml of methanol were heated until the thiourea dissolved. Then 1.5 ml solution of formaldehyde was added, and pH was adjusted to 3 with acetic acid. The mixture was then kept in microwave at 90 °C. The experimental conditions are shown in Table 1.

Table 1. Optimization of reaction conditions for T-F polymer

S.N	Power (W)	Time (min)	Temperature (°C)	Yield (%)
1	300	5	90	10
		10		16
2	400	5	90	18
		10		25
3	500	5	90	32
		10		48
4	700	5	90	65
		10		79

The reaction was monitored by thin layer chromatography (TLC) using ethanol as an eluent. The resulting colourless viscous product was washed with diluted NaOH solution, distilled water, ethanol and acetone [22].



Scheme 1. Synthetic route for the formation of T-F polymer

2.3. Weight loss measurements

Weight loss experiments were performed by immersing the MS coupon in 1M HCl (100 ml) in absence and presence of different concentration of inhibitor. After 3 h of immersion time the coupons were taken out, washed, dried and weighted accurately. The corrosion rate (C_R), inhibition efficiency ($\eta\%$), surface coverage (θ) and were determined by using following equations,

$$C_R (\text{mm/y}) = \frac{87.6W}{atD} \quad (1)$$

$$\eta\% = \frac{C_R - {}^iC_R}{C_R} \times 100 \quad (2)$$

$$\theta = \frac{C_R - {}^iC_R}{C_R} \quad (3)$$

where W is the average weight loss of MS specimens, a is total surface area of MS specimen, t is the immersion time (3 h) and D is the density of MS in (gcm^{-3}), in equation (2) C_R and iC_R is the corrosion rates of MS in the absence and presence of the inhibitors respectively.

2.4. Electrochemical measurements

The electrochemical experiments were performed in conventional three electrode cell, connected to Potentiostat/Galvanostat G300-45050 (Gamry Instruments Inc., USA). Echem Analyst 5.0 software package was used for data fitting. Cell assembly consists of MS as working electrode with

an exposed area of 1 cm^2 , platinum electrode as an auxiliary electrode, and saturated calomel electrode (SCE) as reference electrode. All potentials reported were measured versus SCE. Tafel curves were obtained by changing the electrode potential automatically from -0.25 V to $+0.25 \text{ V}$ versus open corrosion potential at a scan rate of 1.0 mVs^{-1} . EIS measurements were performed under potentiostatic conditions in a frequency range from 100 kHz to 0.01 Hz , with amplitude of 10 mV AC signal. The experiments were carried out after an immersion period of 30 min in 1 M HCl in absence and presence of different concentrations of T-F Polymer.

3. RESULTS AND DISCUSSION

3.1. Electrochemical measurements

3.1.1. Potentiodynamic polarization measurements

The Potentiodynamic polarization curves for mild steel in 1 M HCl in absence and presence of inhibitors are shown in Figure 2 and electrochemical parameters such as corrosion potential (E_{corr}), corrosion current density (I_{corr}), anodic and cathodic slopes (β_a and β_c) obtained from these curves are given in Table 2. The inhibition efficiencies were calculated by I_{corr} values using following equation,

$$\eta\% = \frac{I_{\text{corr}} - I_{\text{corr(inh)}}}{I_{\text{corr}}} \times 100 \quad (4)$$

where I_{corr} and $I_{\text{corr(inh)}}$ are the corrosion current density in absence and presence of inhibitor respectively, in 1 M HCl .

The results of polarization study show that the addition of different concentrations of polymer leads to a decrease in the I_{corr} values [23]. The maximum decrease in I_{corr} values and hence, highest inhibition efficiency (93.5%) was obtained at 600 ppm . It is also observed that the addition of inhibitor causes a significant change in corrosion potential E_{corr} . The presence of polymer causes E_{corr} shifts towards negative direction having maximum E_{corr} obtained 65 mV with respect to blank acid solution, indicating mixed type inhibition [24].

Table 2. Polarization data for MS in 1 M HCl in absence and presence of different concentrations of T-F polymer.

Inhibitors	Concentrations (ppm)	I_{corr} (μAcm^{-2})	E_{corr} (mV/SCE)	β_a (mV/dec)	β_c (mV/dec)	$\eta\%$
Blank	0.0	1070	-448	46	96	-
	100	374	-515	58	298	65.0
	200	221	-514	52	213	79.3
	300	208	-511	46	121	80.5
	400	101	-517	39	68	90.5
	500	91	-503	40	87	91.4
	600	69	-513	29	57	93.5

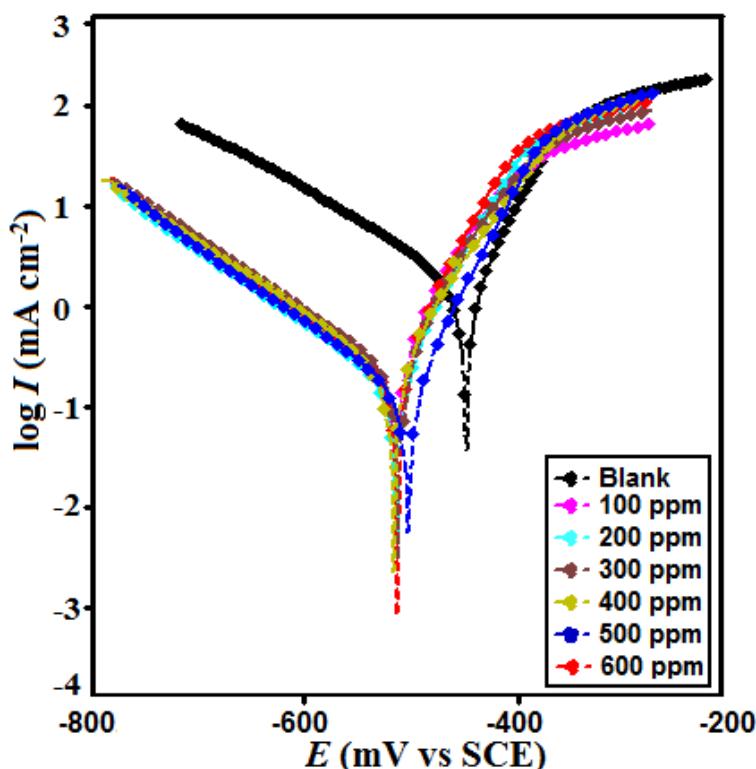


Figure 2. Polarization curves for MS in 1 M HCl in absence and presence of different concentrations of T-F polymer

3.1.2. Electrochemical impedance spectroscopy (EIS)

The Nyquist plot depicts the impedance response of mild steel. From the plots, it can be observed that impedance response of mild steel is increased by the addition of T-F Polymer. The obtained Nyquist plots are not perfect semicircles, which is attributed to non-homogeneity of the surface and roughness of the metal. The Nyquist plot and equivalent circuit model is shown in Figure. 3(a), (b) and corresponding data are given in Table 3.

The capacitive loop indicates that the corrosion of MS is mainly controlled by a charge transfer process and the highest the capacitive loop obtained at 600 ppm. It is seen that addition of T-F Polymer increases the values of R_{ct} and reduces the C_{dl} . The decrease in C_{dl} is attributed to an increase in the thickness of electronic double layer [25-26]. The values of double layer capacitance, C_{dl} was calculated from equation,

$$C_{dl} = Y_0 (\omega_{max})^{n-1} \tag{5}$$

where Y_0 is CPE coefficient, n is CPE exponent (phase shift), ω is the angular frequency.

The thickness of this protective layer (d) is correlated with C_{dl} by the following equation,

$$C_{dl} = \frac{\epsilon\epsilon_0 A}{d} \tag{6}$$

where ϵ is the dielectric constant and ϵ_0 is the permittivity of free space and A is surface area of the electrode.

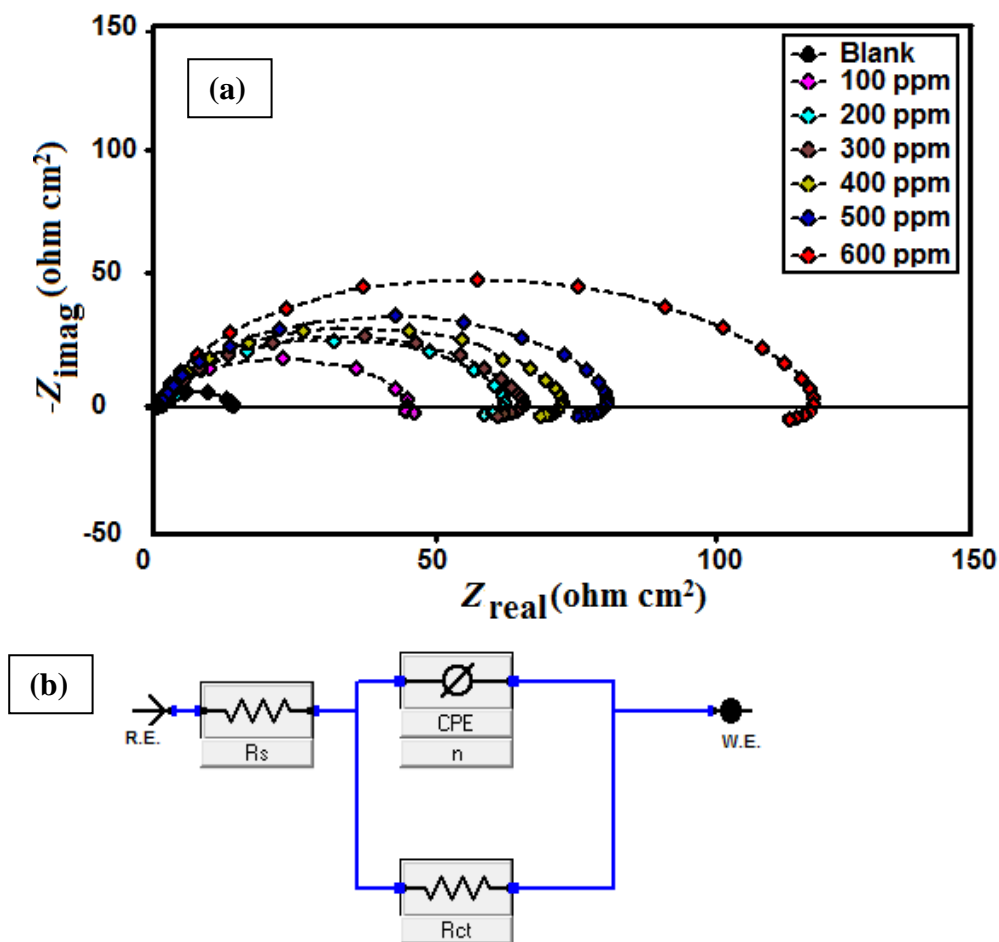


Figure 3. The (a) Nyquist plot and (b) equivalent circuit model for MS in 1M HCl containing different concentrations of T-F polymer

The higher values of R_{ct} are generally attributed to slower rate of corrosion of MS. The inhibition efficiency is calculated using charge transfer resistance (R_{ct}) as follows,

$$\eta\% = \frac{R_{ct(inh)} - R_{ct}}{R_{ct(inh)}} \times 100 \tag{7}$$

Where $R_{ct(inh)}$ and R_{ct} are the values of charge transfer resistance in presence and absence of inhibitor in 1M HCl respectively

Bode plot and phase angle plot are plotted against frequency and a linear relationship between $|Z|$ against $\log f$, with slope near -1 and the phase angle tends to become -90° behave as ideal capacitor. The slope value ($-S$) 0.82 and phase angle ($-\alpha^\circ$) 74.15 are obtained for MS in presence of 600 ppm of T-F Polymer. The deviation from the ideal capacitive behavior is due to electrochemical system which generally does not behave in an ideal manner. The phase angle at higher frequencies is attributed to anticorrosion performance. The more negative the phase angle, the more capacitive the electrochemical behavior [27] shown in Table 4, bode phase angle plot is shown in Figure 4.

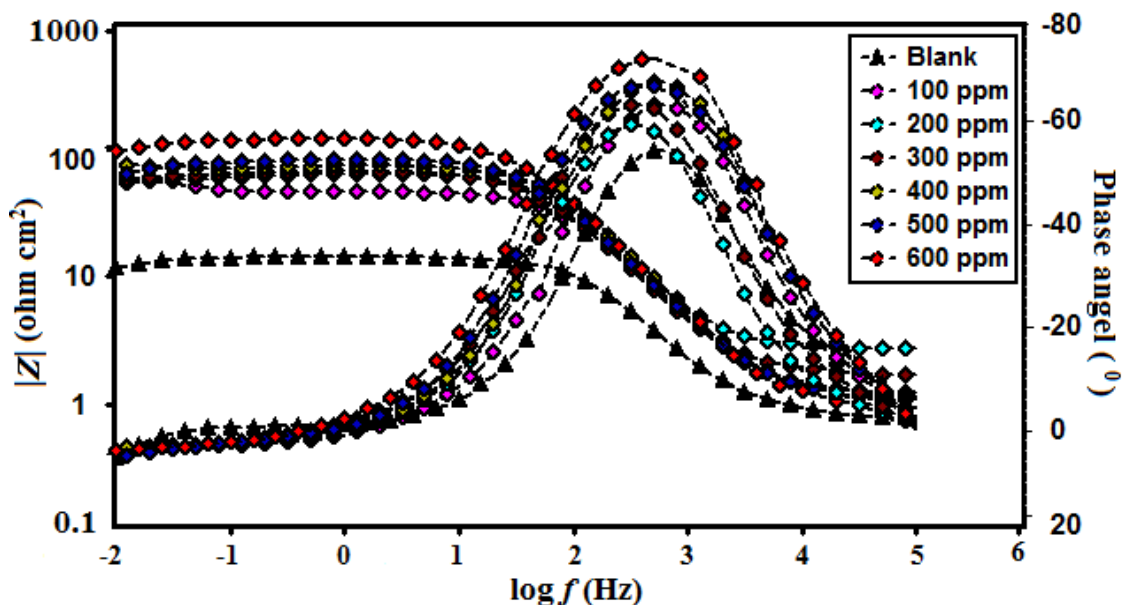


Figure 4. Bode-impedance and Phase angle plots for MS in 1M HCl containing different concentrations of T-F polymer.

Table 3. Electrochemical impedance parameters and corresponding efficiencies of MS in 1M HCl at different concentrations of T-F polymer

Inhibitor concentration(ppm)	R_{ct} ($\Omega \text{ cm}^2$)	n	Y_o ($10^{-6} \Omega^{-1} \text{ cm}^{-2}$)	C_{dl} ($\mu\text{F cm}^{-2}$)	$\eta\%$
Blank	12.1	0.868	242.6	100.6	-
100	42.5	0.897	88.4	46.6	71.5
200	56.0	0.906	80.7	45.9	78.9
300	60.8	0.894	77.6	42.1	80.0
400	69.1	0.902	76.1	41.3	82.4
500	76.9	0.889	74.4	40.4	84.2
600	113.0	0.901	67.2	39.8	89.2

Table 4 Slopes of the Bode plots at Intermediate Frequencies (S) and the Maximum Phase angles (α°) for Mild Steel in 1M HCl solution with increasing T-F polymer concentrations

Inhibitor concentration(ppm)	$-\alpha^\circ$	$-S$
Blank	54.29	0.67
100	63.17	0.73
200	59.29	0.77
300	63.39	0.80
400	67.70	0.84
500	67.19	0.81
600	74.15	0.82

3.2. Weight loss measurements

3.2.1. Effect of inhibitor concentration

The weight loss experiment is a base line method to observe optimum concentration after which there is no remarkable change in the inhibition efficiency. This may be due to the adsorption of T-F Polymer leading to the formation of a smooth layer on metal surface which prevents the contact of metal with the surrounding acidic environment and higher bonding ability of inhibitor on the mild steel surface is due to the higher number of lone pairs on heteroatoms and π orbitals. Data obtained for MS in 1M HCl in presence and absence of different concentrations of inhibitor is summarized in Table 5. The corrosion rate values of MS in 1M HCl decreases as the concentration of T-F Polymer increases [28-29].

Table 5. Weight loss data for MS in 1M HCl at different concentrations of T-F polymer

Inhibitor concentration(ppm)	C_R (mm/y)	θ	η (%)
Blank	74.20	-	-
100	34.87	0.53	53.0
200	26.34	0.64	64.5
300	15.95	0.78	78.5
400	13.72	0.81	81.5
500	7.04	0.90	90.5
600	4.82	0.93	93.5

3.2.2. Adsorption isotherm

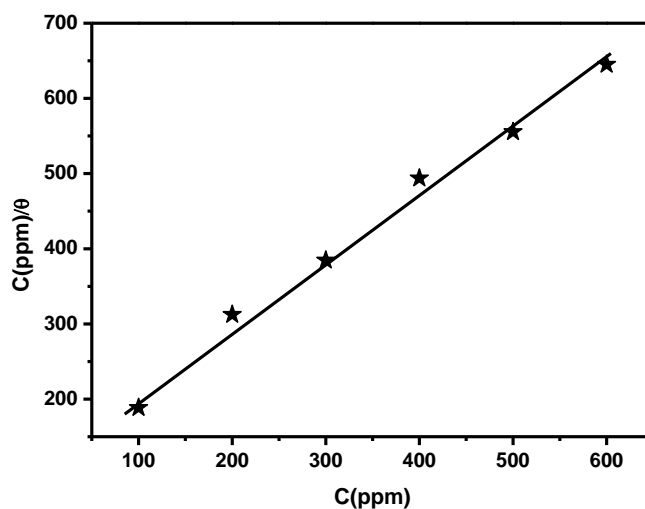


Figure 5. The Langmuir adsorption isotherm plot for MS at different concentrations of T-F polymer.

Adsorption process of an inhibitor depends upon its nature such as planarity of compound lone pairs present in hetro atoms, multiple bonds etc. The addition of T-F Polymer rapidly forms a protective layer on metal surface through metal/solution interface [30-31]. The solid MS surface contains a fixed number of adsorption sites and each site holds one adsorbed species. The surface coverage, θ , covered after adsorption was calculated according to equation (3).

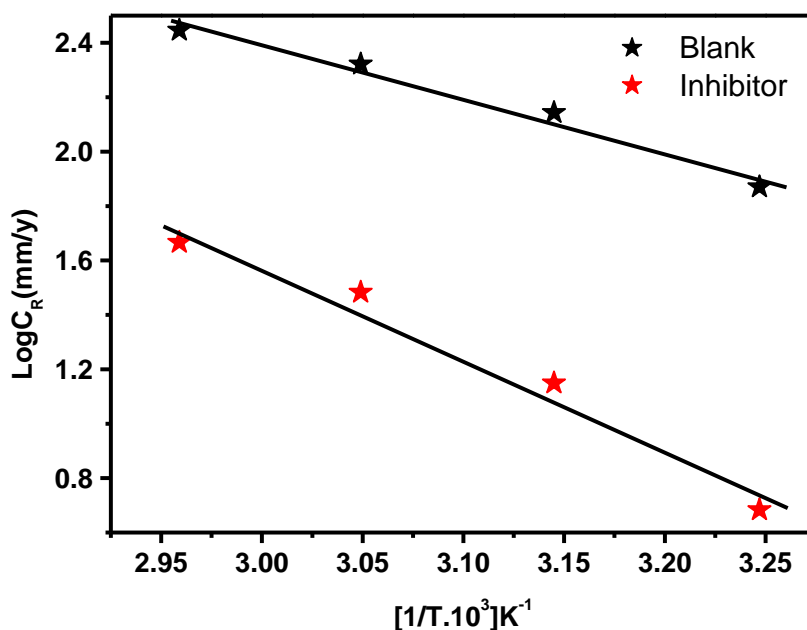
By fitting the degree of surface covered (θ) to adsorption isotherms including Frumkin, Temkin and Langmuir isotherms, best fit was obtained in the case of Langmuir isotherm by plotting (C/θ) vs. θ gives a straight line with regression coefficient ($R^2 = 0.9921$) as shown in Figure 5.

3.2.3. Thermodynamic activation parameters

The effect of temperature can be understood by thermodynamic activation parameters during corrosion process. Activation energy increases with increasing temperature due to decrease in adsorption of T-F Polymer resulting in dissolution of already adsorbed layer [32-33]. As the temperature rises, the metal comes in contact with outward corrosive environment leading to dissolution of metal. The activation energy can be calculated using following equation,

$$\ln(C_R) = \frac{-E_a}{RT} + A \tag{8}$$

where E_a is the activation energy for corrosion of MS in 1M HCl, R is the gas constant, A the Arrhenius pre-exponential factor and T is the absolute temperature. A plot of the corrosion rate $\ln C_R$ vs $1000/T$ gives a straight line as shown in Figure 6(a). The values of E_a in 1 M HCl in absence and presence of T-F Polymer are determined from the slope by plotting the values obtained given in Table 6.



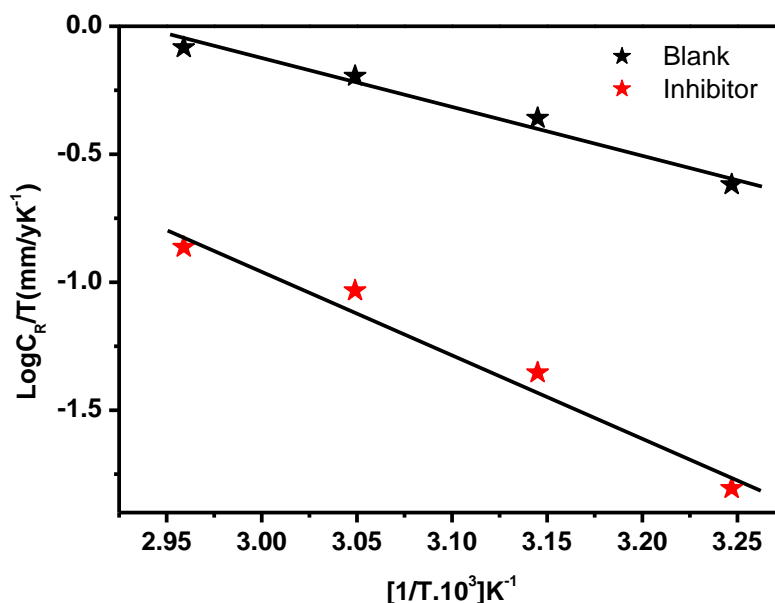


Figure 6. Adsorption isotherm plots (a) $\log C_R$ vs. $1000/T$ (b) $\log C_R/T$ vs. $1000/T$ for MS in 1M HCl in the absence and presence T-F polymer.

A plot of $\ln (C_R /T)$ against $1000/T$ shown in Figure 6(b) which gives straight lines with a slope of $(-\Delta H^*/R)$ and an intercept of $[(\ln(R/Nh)) + (\Delta S^*/R)]$ to which the values of ΔH^* and ΔS^* are calculated and are given in Table 6.

The enthalpy and entropy of activation (ΔH^* and ΔS^*) can be calculated by given equation,

$$C_R = \frac{RT}{Nh} \exp\left(\frac{\Delta S^*}{R}\right) \exp\left(-\frac{\Delta H^*}{RT}\right) \tag{9}$$

Where h is Plank constant and N is Avogadro’s number.

The positive signs of enthalpies (ΔH^*) reflect the endothermic nature of dissolution process. The shift towards positive value of entropies (ΔS^*) shows a decrease in entropy of the solute and increase in entropy of the solvent and disorder increases on going from reactants to the activated complex [34-35].

Table 6. Thermodynamic parameters for mild steel in 1M HCl in absence and presence of T-F polymer.

Inhibitor concentration(ppm)	E_a (kJmol ⁻¹)	ΔH^* (kJmol ⁻¹)	ΔS^* (Jmol ⁻¹ K ⁻¹)
Blank	38.15	35.47	-93.62
600	65.77	63.09	-26.17

3.3. Surface characterization by Optical microscopy

The mild steel surface was examined by Optical microscopy in presence and absence of T-F Polymer in 1M HCl and the results are shown in Figure 7. The fine surface of MS after abrading with different grade of emery paper is shown in Figure 7(a). The mild steel coupon which was dipped in 1 M HCl without inhibitor in Figure 7(b) showed corroded areas on its polished surface which do not exist on the clear sample. The presence of such regions can be attributed to the dissolution of MS due to the surface attack by the aggressive acid solution. The image of MS surface obtained in presence of T-F Polymer shows a protected surface area of metal in Figure 7(c). The presence of inhibitor lowers the corrosion rate of metal due to adsorption of the same on metal surface which protected the metal surface during direct contact with acid solution [36]

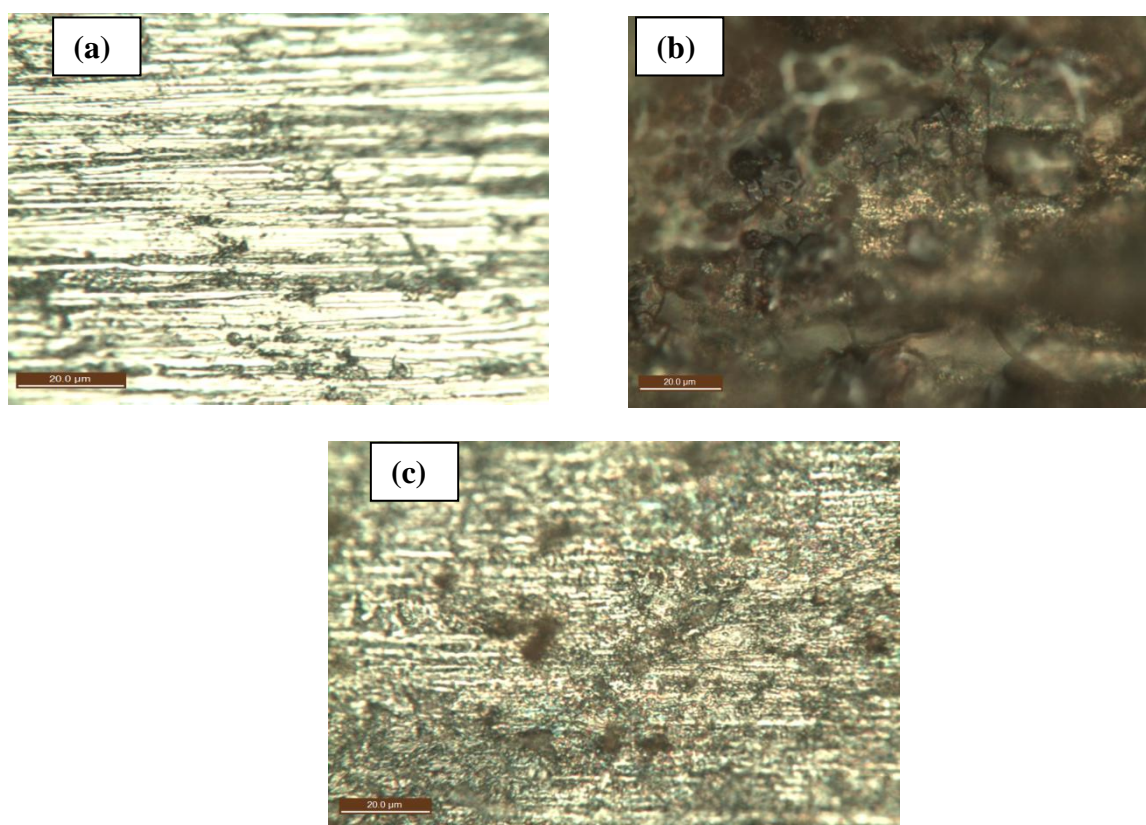


Figure 7. Optical microscopy of (a) Polished mild steel, (b) mild steel in HCl, (c) mild steel in 1M HCl with T-F polymer.

3.4. Mechanism of adsorption and inhibition

Adsorption of T-F polymer on metal surface depends on parameters such as mode of adsorption, active sites on metal surface, planarity of molecules, free lone pairs present on heteroatoms, concentration of inhibitor etc. Normally the adsorption of inhibitor on metal surface and formation of protective layer to prevent corrosion can be understood by three ways. The first is the electrostatic interaction of protonated inhibitor molecules with already adsorbed chloride ions

(physisorption). At lower concentration, protonated molecules get adsorbed on the surface of mild steel through electrostatic interaction. With increasing concentration protonated inhibitor molecules turn to neutral molecules due to slower rate of hydrogen evolution having free lone pair electrons and promote chemical adsorption. Second way deals with the free lone pairs of heteroatoms and vacant d orbitals of Fe of mild steel (chemisorption). Third method is the interaction of d-electrons from Fe of mild steel with the vacant orbital of inhibitor molecule (reterodonation) [37-38] as shown in Figure 8.

The inhibitor molecules having d orbital electrons have both the tendency to donate and to accept free electrons and form stable chelates which behave like effective inhibitors. The presence of S-atom in the T-F Polymer forms $d\pi-d\pi$ bond resulting in transfer of 3d-electrons from Fe atom to the vacant 3d orbital of S-atom, which enhances adsorption process on metal surface due to strong back bonding. The studied polymer has hetero atoms containing long chain, which adsorbed on metal surface and form a thick layer to prevent direct contact of metal with aggressive media or to slow down corrosion rate of metal [39].

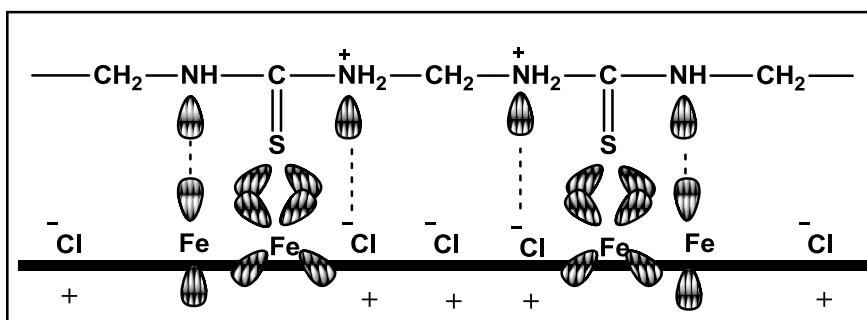


Figure 8. Pictorial representation of mechanism of adsorption of T-F polymer on MS surface

4. CONCLUSIONS

1. T-F Polymer acts as good inhibitors for the corrosion of mild steel in 1M HCl.
2. Potentiodynamic polarization measurements studies show that investigated T-F polymer behaves as mixed-type inhibitor.
3. EIS plots indicated that R_{ct} values increase and C_{dl} values decrease with increasing T-F polymer concentration.
4. The adsorption of the inhibitor molecules on the mild steel surface was found to obey the Langmuir adsorption isotherm. All these data support good inhibition tendency of T-F Polymer.

ACKNOWLEDGEMENTS

Priyanka Singh is thankful to University Grants Commission (UGC), New Delhi for the Project (40-101/2011) SR, Fellowship.

References

1. S.A. Umoren, O. Ogbobe, I.O. Igwes, E.E. Ebenso, *Corros. Sci.* 50 (2008) 1998

2. P. Singh, A. Singh, M.A. Quraishi, E.E. Ebenso, *Int. J. Electrochem. Sci.* 7 (2012) 7065
3. P. Singh, A. Singh, M.A. Quraishi, E.E. Ebenso, *Int. J. Electrochem. Sci.* 7, (2012) 8612
4. F.S. De Souza, A. Spinelli, *Corros. Sci.* 51 (2009) 642
5. M.M. El-Naggar, *Corros. Sci.* 49 (2007) 2226
6. S.E. Nataraja, T.V. Venkatesha, H.C. Tandon, B.S. Shylesha, *Corros. Sci.* 53 (2011) 4109
7. S.K. Shukla, M.A. Quraishi, *Corros. Sci.* 51 (2009) 1007
8. Z. Tao, S. Zhang, W. Li, B. Hou, *Corros. Sci.* 51 (2009) 2588
9. S. Zhang, Z. Tao, W. Li, B. Hou, *Appl. Surf. Sci.* 255 (2009) 6757
10. C. Kamal, M.G. Sethuraman, *Arabian J. Chem.* 5, (2012) 155
11. K.F. Khaled, S.S. Abdel-Rehim, G.B. Sakr, *Arabian J. Chem.* 5 (2012) 213
12. A. Yurt, S. Ulutas, H. Dal, *Appl. Surf. Sci.* 253 (2006) 919
13. S.M.A. Hosseini, A. Azimi, *Corros. Sci.* 51 (2009) 728
14. F. Bentiss, C. Jama, B. Mernari, H El. Attari, L El. Kadi, M. Lebrini, M. Traisnel, M. Lagrenee, *Corros. Sci.* 51(2009) 1628
15. H. Bhandari, R. Srivastav, V. Choudhary, S.K. Dhawan, *Thin Solid Films* 519 (2010) 1031
16. S.K. Shukla, M.A. Quraishi, R. Prakash, *Corros. Sci.* 50 (2008) 2867
17. Y. Ren, Y. Luo, K. Zhang, G. Zhu, X. Tan, *Corros. Sci.* 50 (2008) 3147
18. G. Achary, Y.A. Naik, S.V. Kumar, T.V. Venkatesha, B.S. Sherigara, *Appl. Surf. Sci.* 254 (2008) 5569
19. M.M. Solomon, S.A. Umoren, I.I. Udoso, A.P. Udoh, *Corros. Sci.* 52 (2010) 1317
20. S.S. Abd El Rehima, S.M. Sayyah, M.M. El-Deeb, S.M. Kamal, R.E. Azooz, *Mater. Chem. Phys.* 123 (2010) 20
21. S.K. Shukla, M.A. Quraishi, *J. Appl. Polym. Sci.* 124 (2012) 5130
22. T. Ahamad, V. Kumar, N. Nishat, *Polym. Int.* 55 (2006) 1398
23. G. Ji, S.K. Shukla, P. Dwivedi, S. Sundaram, R. Prakash, *Ind. Eng. Chem. Res.* 50 (2011) 11954
24. S.K. Shukla, A.K. Singh, I. Ahamad, M.A. Quraishi, *Mater. Lett.* 63, (2009) 819
25. I. Ahamad, R. Prasad, M.A. Quraishi, *Corros. Sci.* 52 (2010) 3033
26. M.A. Amin, S.S. Abd El Rehim, H.T.M. Abdel-Fatah, *Corros. Sci.* 51 (2009) 882
27. D.K. Yadav, M.A. Quraishi, *Ind. Eng. Chem. Res.* 51, (2012) 8194
28. E.E. Oguzie, C.K. Enenebeaku, C.O. Akalezi, S.C. Okoro, A.A. Ayuk, E.N. Ejike *J. Colloid Interface Sci.* 349 (2010) 283.
29. G. Achary, H.P.Sachin, Y.A. Naik, T.V. Venkatesha, *Mater. Chem. Phys* 107 (2008) 44
30. S. Banerjee, V. Srivastava, M.M. Singh, *Corros. Sci.* 59 (2012) 35
31. A.K. Singh, S.K. Shukla, M.A. Quraishi, E.E. Ebenso, *J. Taiwan Inst. Chem. Eng.* 43 (2012) 463
32. G. Achary, Y.A. Naik, S.V. Kumar, T.V. Venkatesha, B.S. Sherigara, *Appl. Surf. Sci.* 254 (2008) 5569
33. M. Behpoura, S.M. Ghoreishia, M. Khayatkashania, N. Soltani, *Mater. Chem. Phys* 131 (2012) 621
34. Z. Tao, W. Hea, S. Wang, S. Zhang, G. Zhou, *Corros. Sci.* 60 (2012) 205
35. D.K. Yadav, B. Maiti, M.A. Quraishi, *Corros. Sci.* 52 (2010) 3586
36. Dae-K. Kim, S. Muralidharan, Tae-H. Ha, Jeong-H. Bae, Yoon-C. Ha, Hyun-G. Lee, J.D. Scantlebury, *Electrochim. Acta* 51 (2006) 5259
37. B.S. Sanatkumar, J. Nayak, A. N. Shetty, *Int. J. Hydrogen Energy* 37 (2012) 9431
38. I. Ahamad, C. Gupta, R. Prasad, M.A. Quraishi, *J Appl. Electrochem.* 40 (2010) 2171
39. I. Ahamad, R. Prasad, M.A. Quraishi, *Corros. Sci.* 52 (2010) 1472